PROBLEMY MECHATRONIKI
UZBROJENIE, LOTNICTWO, INŻYNIERIA BEZPIECZEŃSTWA

ISSN 2081-5891

10, 4(38), 2019, 71-86

PROBLEMS OF MECHATRONICS
ARMAMENT, AVIATION, SAFETY ENGINEERING

35 "Ur" Type Anti-Tank Rifle – A Numerical Analysis of Armour Penetration of a World War II Tank

Mariusz MAGIER[1*], Paweł ŻOCHOWSKI[1], Wojciech BURIAN[2]

[1]Military Institute of Armament Technology,
7 Prymasa Stefana Wyszyńskiego Str., 05-220 Zielonka, Poland
[2]Łukasiewicz Research Network - Institute of Non-Ferrous Metals
5 Sowińskiego Str., 44-100 Gliwice, Poland
[*]Corresponding author's e-mail address and ORCID:
magierm@witu.mil.pl; https://orcid.org/0000-0002-4431-9537

Received by the editorial staff on 27 August 2018
The reviewed and verified version was received on 4 December 2019

DOI 10.5604/01.3001.0013.6487

Abstract. The paper presents a simulated process of penetration of a steel slab with a strength performance approximate to that of World War II battle tanks with a 7.92 mm DS projectile fired from the 35 "Ur" type anti-tank rifle. The basic technical parameters necessary for the simulation process were sourced from historical records. The FEM (*Finite Element Method*) applied in LS-Dyna enabled an estimation of the penetrating capability of the DS projectile. Decisive to the high penetrating capability of the DS projectiles were the non-optimized properties of armour steel (its high brittleness) and a high kinetic energy of the projectile, which generated high shearing stresses upon impact against the steel slab causing the effect of 'plugging' upon penetration.

This work has been compiled from the paper presented during the 12th International Armament Conference on Scientific Aspects of Armament & Safety Technology, Jachranka, Poland, September 17-20, 2018.

The numerical simulation results confirmed the high combat effectiveness of the DS projectile and the argument that the DS projectile could pierce a 20 mm thick armour plate made from the material applied during the World War II era.
Keywords: anti-tank rifle, armour, terminal ballistics, FEM

1. INTRODUCTION

The year 1916 saw the first combat application of tanks on the battlefields of the Great War. Initially, the then tanks were fought with field artillery, designed to shoot along a straight-line trajectory. However, field artillery was not a standard issue of the infantry; it was assigned to artillery units which provided fire support for other branches of the military. Hence, it was difficult to provide full anti-armour protection of infantry units faced with an armoured offensive.

As early as in 1918, Germans began the development of an anti-tank rifle based on the 7.9 mm calibre Mauser infantry rifle. The new weapon entered serial production in May 1918 under the name *Mauser Tank-Gewehr M1918*. The anti-tank rifle had a poor rate of fire and a high force of recoil, by which it earned its infamous nickname: *"The Collar-Bone Breaker"*. With a calibre of 13.25 mm, the anti-tank rifle weighed 16.6 kg (Fig.1). The muzzle velocity of the projectile was 785 m/s. The projectile had a solid steel core with a weight of 51.5 g and could penetrate a 25 mm thick steel slab from a firing distance of 100 m [1].

Fig. 1. M1918 13.25 mm calibre anti-tank rifle (courtesy: Royal Armouries)

Further and better-known anti-tank designs were developed right before World War II. The German PzB38 7.92x94 mm calibre anti-tank rifle (Fig.2) entered serial production in 1938. Due to a complicated design of the breech mechanism, it saw infrequent combat use in the Wehrmacht (a total of approximately 1400 units were made). The weapon's weight was 16.2 kg. The muzzle velocity of the projectile was 1210 m/s. The projectile could penetrate a 25 mm thick steel slab from a firing distance of 100 m [2]. A modified (and simplified) version of the anti-tank rifle entered service under codename PzbB39. A total of over 39,000 units were made.

Fig. 2. PzB38 7.92 mm calibre anti-tank rifle (courtesy: Bundesarchiv)

An anti-tank rifle under codename Lahti L-39 (Fig.3) was developed and entered serial production in 1939 in Finland. It saw its first combat application during the Winter War between Finland and the Soviet Union. Each unit of this 20 x 138 mm calibre weapon weighed nearly 50 kg.

The projectile with a muzzle velocity of 800 m/s and an approximate weight of 120 g could penetrate a 20 mm thick steel plate from a distance of 300 m [3].

In 1937, the popularly named Boys anti-tank rifle (Fig.4) was officially listed in the armament of the British military. With a calibre of 13.97 mm and a weight of 16 kg, the weapon was developed to counter the challenging and dynamic growth of German armoured forces in the 1930s.

Fig. 3. Lathi L-39 20 mm calibre anti-tank rifle (courtesy: Joonas Tupala, 2015)

Depending on the production version, the muzzle velocity of the projectile varied from 747 m/s (for a 61-gram solid steel core projectile) to 945 m/s (for a 48 g tungsten core projectile). The penetrating capability of the Mark II solid steel core projectile (muzzle velocity 884 m/s) was 23.2 mm of armour at a firing distance of approximately 100 yards (91 m).

Fig. 4. Boys 13.97 mm calibre anti-tank rifle
(courtesy: http://weaponsman.com)

2. CHARACTERISTICS OF THE 35 "UR" TYPE ANTI-TANK RIFLE

The 35 type anti-tank rifle (Polish abbreviated nomenclature: kb ppanc wz. 35), codename "Ur" (alternatively, "kb Ur") was developed by a weapons design engineering team led by Józef Maroszek in the middle of the 1930s. The weapon saw its serial production in 1938 (Fig.5). Each unit with a weight of 9.5 kg was fed with a single-row box magazine with a capacity of four ammunition rounds. The interchangeable barrel featured a muzzle brake with an efficiency of 65%. The service life of the barrel was approximately 300 shots.

Fig. 5. 7.92 mm calibre 35 type anti-tank rifle (courtesy: Wikimedia Commons)

Unlike the anti-tank rifles showcased before, the 35 "Ur" type was fed with soft lead core ammunition rounds (7.92 × 107 mm DS, Fig.6)), instead of solid steel core rounds. The lead core resulted in a lower risk of ricocheting upon impinging the armour surface at an angle from the perpendicular. Depending on the armour plate thickness and the kinetic energy of the DS projectile, it could blow a "plug" with an approximate diameter of 20 mm through the plate upon penetration. If fragmented, the armour plate plug could strike the armoured vehicle's crew and internal components.

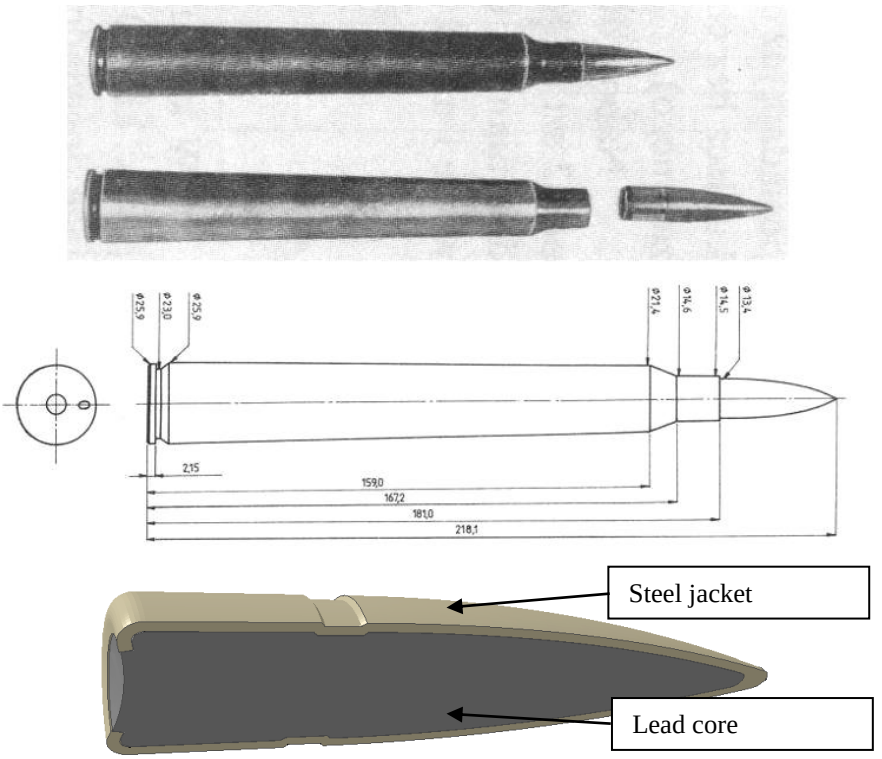

Fig. 6. 7.92 x 107 mm cartridge with the DS projectile
(courtesy: http://www.dws-xip.pl)

If the DS projectile failed to penetrate armour, it would deform on its outer surface and transmit a part of the kinetic energy to the plating. This in turn could cause delamination of the armour plate and its fragmentation at force to the inside of the armoured vehicle. With a high muzzle velocity (of 1275 m/s maximum) and a weight of 14.6 g, the DS projectile could penetrate a 33 mm thick steel plate at a firing distance of 100 mm [4-6].

3. NUMERICAL ANALYSIS OF THE DS PROJECTILE IMPACT AGAINST ARMOUR PLATING

During the penetration of the armour plate, the soft lead core would reveal a plastic flow and deformation which significantly increased the projectile's diameter. The shearing stresses developed within the armour plate upon impact of the projectile caused 'plugging', which means driving and breaking out a shorn piece of the armour plate with a diameter which, according to reference sources, could achieve three times the original calibre of the projectile [4-6].

The high probability of 'plugging' the armour plate was partially a result of the mechanical properties of armour steel used during the World War II era. According to the material test results from the references [7, 8], which concern steel plates used in the construction of the German PzKw Panther middle tank from World War II, the armour steel used in the era reached a yield stress of R_e = 800-850 MPa and an approximate tensile strength of R_m = 1000 MPa. A characteristic feature of the steel that was important to their shielding capability was low impact strength, especially at high rates of strain.

This resulted in a relatively high proneness to spalling, plugging and generation of many fragments upon ballistic impact. The fragments had a high initial velocity and a high piercing force which allowed striking the interior of the armoured vehicle and its crew. A drawback of lead core projectiles is the steep reduction in penetrating capability with the loss of impact velocity. Below a lower velocity limit characteristic of a specific projectile-armour plate system, the lead core would become completely flattened over the surface of the armour plating and completely fail to penetrate the latter.

The reference sources [4÷6] state that the DS projectile fired from the 35 "Ur" type was capable of penetrating a 15 mm thick steel armour plate positioned at a firing distance of 300 mm and at α=30° to the normal of the armour surface. At a firing distance of 100 mm, the DS projectile could penetrate 33 mm of armour steel. As the standard armour plating thickness ranges of German and Soviet tanks were 7-30 mm and 15-20 mm, respectively, and the steel grades lacked optimized performance characteristics (i.e. they were brittle upon impact with a high rate of strain), an assumption is viable that the 7.92 mm DS projectile fired from the 35 "Ur" type was capable of penetrating the armour plating of any tank contemporary to the weapon.

To gather a thorough insight, understanding and confirmation of the steel armour penetration mechanism of the DS projectile fired from the. 35 "Ur" type anti-tank rifle, three-dimensional numerical analysis was running with the application of FEM (*Finite Element Method*) and an explicit solver in a commercial software suite called LS-Dyna. The system investigated by way of the numerical simulation and analysis is shown in Fig. 7.

The simulated phenomenon was the process of penetrating a 20 mm thick steel slab by the 7.92 mm DS armour-piercing projectile.

Two types of element formulations were applied to specify the individual components of the numerical simulation. The solid elements in a Lagrange formulation (LS-Dyna interface tab *SECTION_SOLID) were applied with suitable erosion criteria to specify the armour (steel) plate and the projectile shell. The three-dimensional digitization of the simulation components is shown in Figures 7 and 8. It was processed in HyperMesh [12]. All simulation components were designed with eight-node elements with reduced integration and the Hourglass element controlled by rigidity (LS-Dyna tab *HOURGLASS).

The element size was selected to prevent the number of elements from extending the processing speed too much on the one hand and enable a precise mapping of the geometry of solids and accurate simulation results on the other. To reduce the number of elements in the simulated armour plate model, the mesh was made denser around the zones of significant strain (the projectile impact point). The spacing between each two adjacent mesh nodes was approximately 0.3 mm at the zones of projectile effect on the armour (with 64 elements along the armour thickness) and increased to 5 mm at the non-strained locations of the armour (with 4 elements along the armour thickness). Ultimately, the armour plate and the projectile shell were specified with 500000 and 95000 finite elements, respectively.

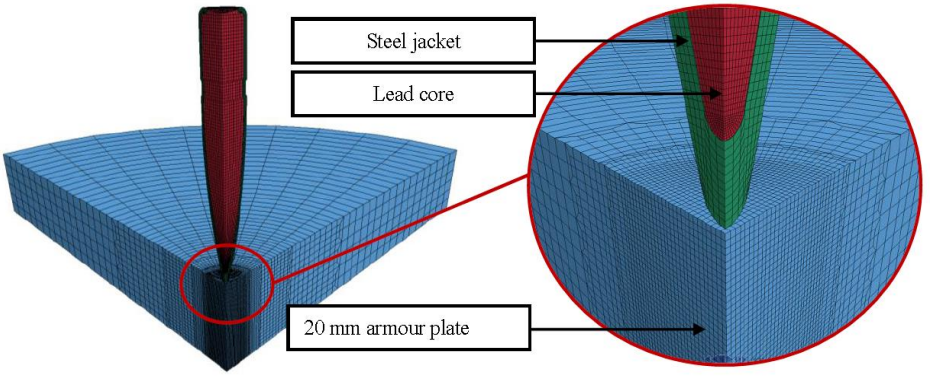

Fig. 7. View of ¼ of the cross-section of the numerical model of the simulated phenomenon expressed with Lagrange formulation and complete with the digitization scheme

A different digitization method was applied to the lead core of the DS projectile. The behaviour of lead under high strain and high strain rates was difficult to map. The application of Lagrange formulation would usually deliver erroneous results; given the high level of deformation of the finite elements of the projectile core, a large number thereof would have to be removed from the model to enable further numerical calculations. This, in turn, would remove a certain mass of the simulated projectile and a certain portion of its kinetic energy, which would overrate the shielding capability of the armour. It was decided to specify the DS projectile core with ALE-formulated finite elements (LS-Dyna tab *SECTION-ALE). For this purpose, the projectile core mesh was designed with a domain, where the latter served as the air encapsulating the core (Fig. 8). Next, the meshes of both components were merged and duplicated nodes were removed (Fig. 9). By the application of the ALE formulation it was possible to model only a small space around the DS projectile core; tab *ALE-REFERENCE_SYSTEM_GROUP available for this method enabled the movement of the domain in concert with the projectile and resizing the domain.

This would not be possible with a standard Euler formulation; the whole space in which the analysed material (the lead core) would be expected to be present in would have to be modelled. Such an approach would require significantly more computing power.

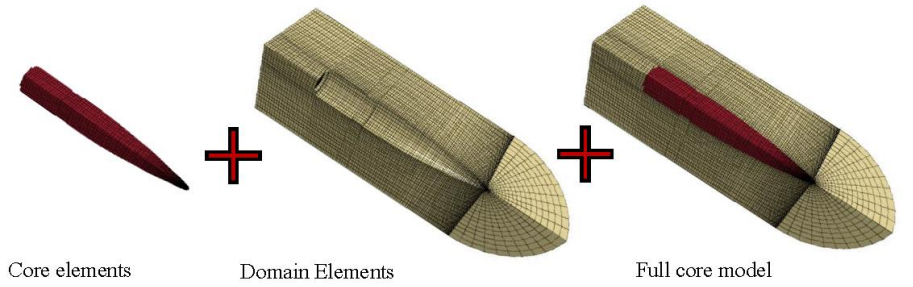

Fig. 8. View of ¼ of the cross-section of the projectile core numerical model with its surrounding in the ALE formulation

Ultimately, the projectile core and its surrounding domain were specified with 39000 and 126000 finite elements, respectively.

The initial boundary conditions were set to make the numerical model most faithful to the features of the simulated system during a real-life phenomenon.

The initial (muzzle) velocity applied to the DS projectile was v_0=1250 m/s (LS-Dyna tab *INITIAL_VELOCITY), and the armour plate was constrained by its circumference (LS-Dyna tab *BOUNDARY_SPC_SET).

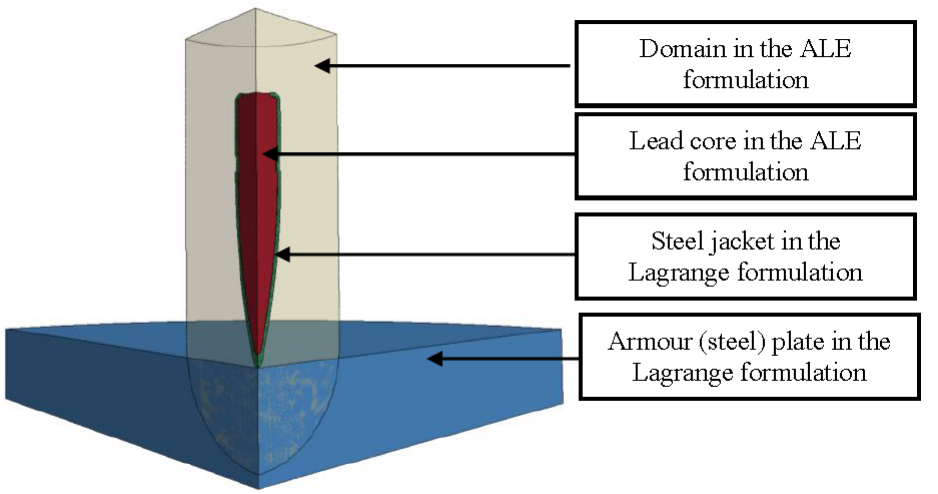

Fig. 9. View of ¼ of the cross-section of the final numerical model of the phenomenon to be calculated

For the Lagrange-formulated elements, the contacts between the individual fragments of the same solid were processed with a model specified in tab *CONTACT_ERODING_SINGLE_SURFACE. To map the interactions between several solids, a contact model *CONTACT-ERODING_SURFACE_TO_SURFACE was used. The interactions between the Lagrange-formulated and ALE-formulated elements were processed with tab *CONSTRAINED_LAGRANGE_IN_SOLID. To eliminate the penetration between the surfaces of the individual simulation components, the minimum fraction of material for contact detection was reduced (FRCMIN=0.1). In all the foregoing contact algorithms, a method was applied based on the "penalty function" [10]. By this method, the solids in contact with one another were classified as master solids and slave solids. The distance between the slave solid nodes and the master solid surface was tested in the direction normal to the segment of the master solid.

If penetration was detected, a force to counter the penetration was generated between the respective node of the slave solid and its point of contact on the master solid surface. The force magnitude depended on the penetration value and the properties of the solids in contact.

Two types of material models were used to properly describe the constitutive relations of the materials in the numerical analysis:

- a plastic material model with kinematic enhancement (*MAT_003) for the DS projectile lead core;
- a modified Johnson-Cook model (*MAT_107) for the armour steel plate and the DS projectile steel shell [9].

The armour plate model had a Cockcroft-Latham (CL) failure model applied [10]. The CL model was based on the value of effort (work) of plastic strain per unit of volume and was expressed by this equation [10]:

$$D = \frac{W}{W_{CR}} = \frac{1}{W_{CR}} \int_0^{\varepsilon_f} \langle \sigma_1 \rangle d\varepsilon_{eq} \tag{1}$$

with: W – level of failure; W_{CR} – CL critical parameter (material constant): when the effort (work) of plastic deformation per unit of volume reached this value, the affected components was qualified as eroded and removed from the numerical simulation; σ_1 – maximum primary stress $\langle \sigma_1 \rangle = \sigma_1$ if $\sigma_1 \geq 0$ and $\langle \sigma_1 \rangle = 0$ while $\sigma_1 < 0$; ε_{eq} – plastic deformation; ε_f – failure strain.

The CL criterion was an assumption that the failure was accumulated during strain until the critical value of $W = W_{CR}$ was achieved. The failure occurred if $W = W_{CR}$ and $\varepsilon_{eq} = \varepsilon_f$; hence, the failure depended both on the applied stresses and the resulting strain. Moreover, the plastic fracture depended on the shearing stresses and the tensile stresses.

The CL criterion was especially interesting in that it enabled results approximate to actual experimental results while having only one failure parameter, W_{CR} , which could be determined by tensile testing.

In the numerical analysis contemplated herein, the value of the parameter was set at W_{CR} = 150 MPa [10], given the brittleness of armour steel referred to in [4-6]. Moreover, the material models of the armour plate and the DS projectile steel shell had erosion algorithms applied (LS-Dyna tab *MAT_000-ADD_EROSION) based on suitable limit values of stress and strain which could emerge in the materials. When an element reached the stress/strain limit, it was removed from the calculations. This eliminated the problem of degenerated elements which would contribute to a reduction of computing speed of the simulation or prevent their continuation altogether.

The data for the numeric models were taken from the reference literature (the lead core and the failure model of the DS projectile shell) and a proprietary material data library developed from proprietary research into the characterisation of materials (for all remaining simulation components). The list of applied parameter values is shown in Table 1.

Figure 10 shows the stress vs. strain curve for the armour plate steel in quasi-static conditions ($\dot{\varepsilon}^*$=1s^{-1}) at room temperature (T=23°C). The curve was plotted from the J-C model equation with the applied parameter values (confined to the plastic interval).

Table 1. Parameter values for the J-C models

Parameter	Steel shell	Armour plate	Parameter	Lead [14]
ρ (g/cm^3)	7.85	7.85	ρ (g/cm^3)	11.35
E (GPa)	210	210	E (GPa)	13.8
v	0.33	0.33	v	0.42
C_p (J/kgK)	4770	4770		
T_m (K)	1800	1800		
Strength model	J-C			*MAT_003
A (MPa)	448	850	R_e	11
B (MPa)	303	150	β	0
n	0.15	0.6	C	-
C	0.003	0.003	P	-
m	1.03	1.05	ε_f	-
Failure model	JC [15]	CL		-
D_1	0.54	150		
D_2	4.88			
D_3	-3.03			
D_4	0.014			
D_5	1.12			
*MAT_ADD EROSION	VOLEPS=0.2 EPSSH =1	EPSSH =1		-

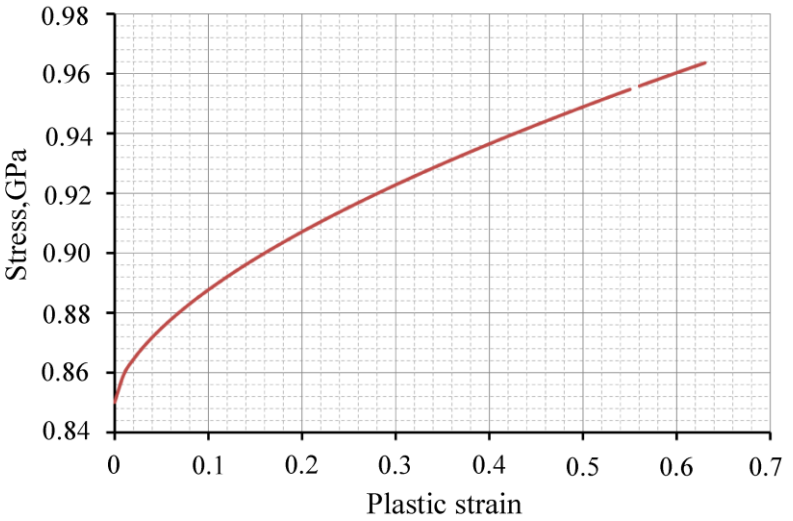

Fig. 10. Stress vs. strain curve plotted for the armour plate steel with the J-C model equation and the applied parameter values (confined to the plastic interval) in quasi-static conditions ($\dot{\varepsilon}^{*}$=1s^{-1}) and at room temperature (T=23°C)

The numerical analysis results, i.e. the condition of the simulation components at specific times of the impact and relative to the initial velocity of the DS projectile are shown in Fig. 12. The numerical analysis runs helped identify the mechanism decisive to the failure of the armour plate during penetration by the DS projectile. The presence and intensity of the individual mechanisms depended on the impact velocity, the shape of the projectile, the projectile diameter to armour thickness relation, and the materials of the target and the penetrator. Given the specific properties of armour steel grades used for the armour plating of combat vehicles in the WW II era considered herein (the close values of yield limit and tensile strength and the reference low impact strength), the armour steel could be classified as a semi-brittle material. The shape of the lead core of the DS projectile changed from an ogive to a sphere during the penetration. Given the foregoing, it was expected that the penetration process would be dominated by the mechanisms of plugging and spalling [11] shown schematically in Fig. 11 [11].

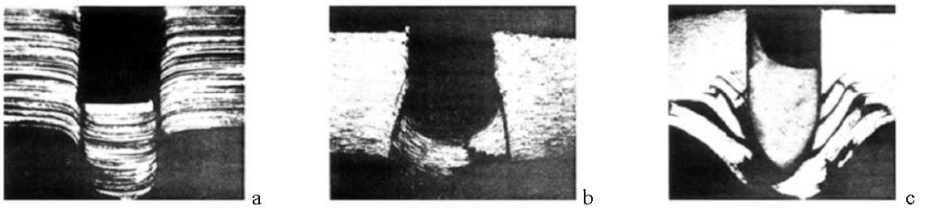

Fig. 11. Mechanisms of armour plating failure by armour-piercing projectiles [11]

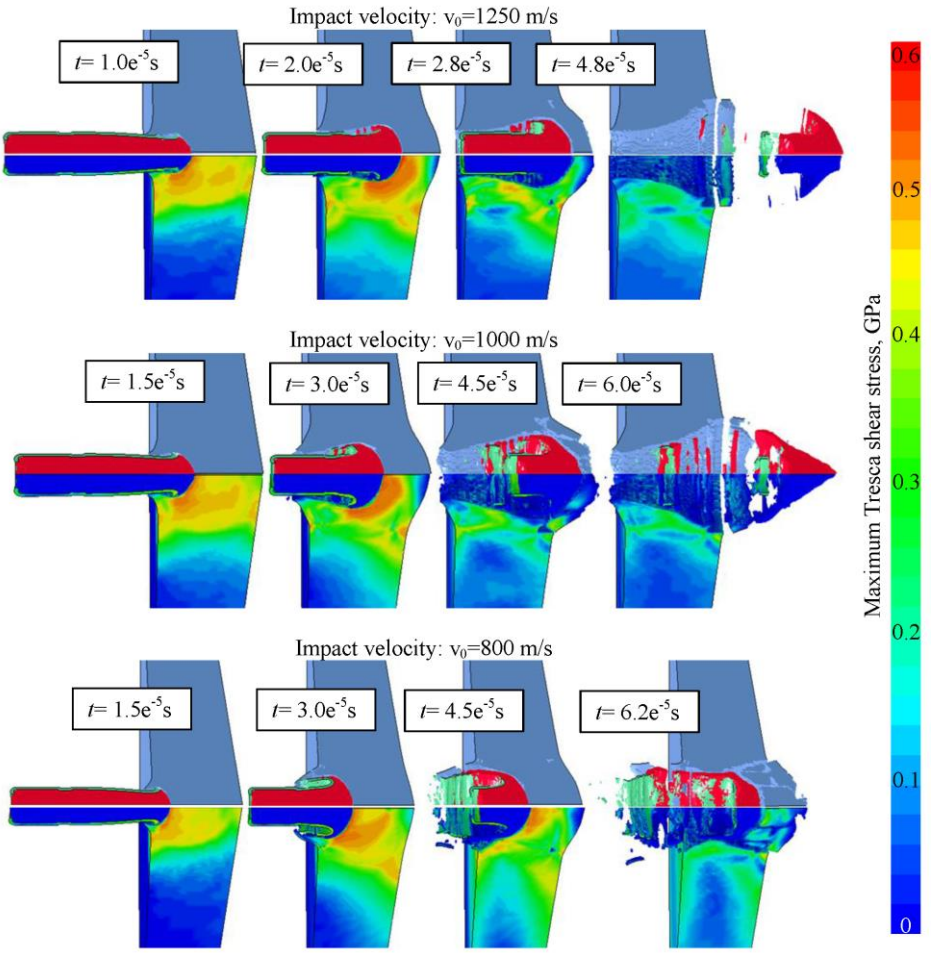

Fig. 12. The conditions of the simulation components at specific times of the phenomenon in relation to the initial velocity of the DS projectile

The numerical analyses proved that three basic and repeatable — albeit different — mechanisms of projectile-to-armour interaction could be classified by impact velocity. The initial stages of penetration were similar for all three mechanisms. The DS projectile was systematically decelerated by the armour plate material, which itself was propelled at the initial stages of plastic strain. By the forces of armour plate reaction, the lead core of the DS projectile was deformed into the characteristic 'mushroom-like' shape, which increased the interface of interaction between the DS projectile and the armour plate.

With the maximum velocity of 1250 m/s of the DS projectile fired from the 35 "Ur" type, the highest bulge in the armour was found due to plastic deformation. For the high kinetic energy of the DS projectile coupled with the reduction of the cross-section of the armour plate, once a limit value was reached, the armour plate material lost integrity and the back layer of the armour plate was spalled and broken into a large number of fragments. The exit hole in the armour plate was much larger than the entry hole. The deformed core of the DS projectile and the armour plate fragments would cause a severe hazard of fatal injury to the crew sheltered by the armoured vehicle hit with the 35 "Ur" type.

Upon impact of the DS projectile with a velocity of 1000 m/s, the penetration mechanism was similar to the foregoing, although the back layer of the armour plate was spalled into a smaller number of fragments, and those were larger than the fragments produced by the first mechanism. Here, a much higher percentage of the initial kinetic energy of the DS projectile was converted into the effort (work) of plastic strain of the armour plate.

However, this time the plastic strain values of the armour plate were lower, as proven by a smaller bulging of the armour plate. This was due to a higher concentration of stresses which, as the bulging grew, became shearing stresses located within the outer circumference of the deformed core of the DS projectile.

The third armour piercing mechanism was different from the foregoing two at the impact velocity of the DS projectile of 800 m/s. The lead core of the DS projectile was completely flattened within the armour steel plate, transferring a considerable fraction of kinetic energy. Before a plug was made, only a small bulge on the rear side of the armour plate was observed. When the failure limit of the C-L model was reached, the affected elements were eroded; the formed cracks propagated from the back surface of the armour plate to the surface of the DS projectile, which caused plugging.

Figure 13 shows the curves plotted for the average projectile core velocity versus time and for different impact velocities.

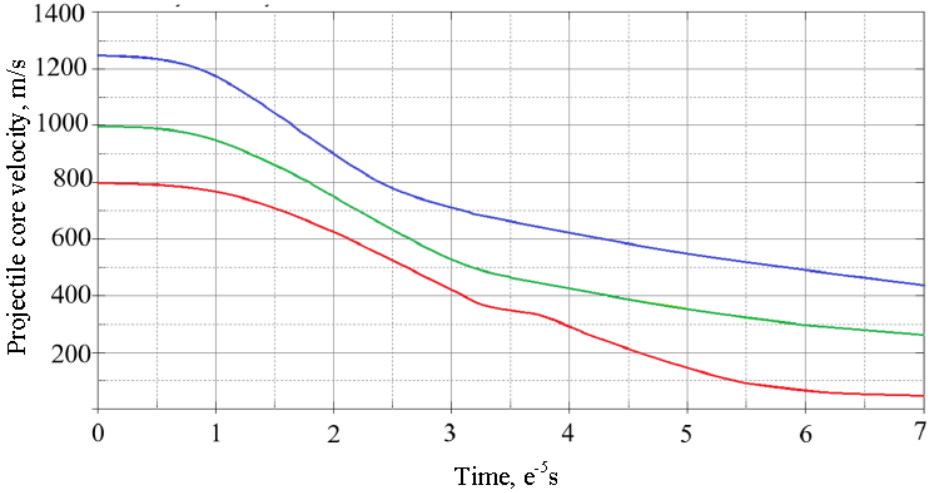

Fig. 13. Average projectile core velocity versus time and for different impact velocities

The chart leads to a conclusion that the velocity of the plug punched by the DS projectile was approximately 50 m/s. The impact velocity of 800 m/s was close to the limit velocity v_{50} (the minimum impact velocity at which the armour plate was pierced) in the projectile-armour plate system analysed here.

4. CONCLUSION

Numerical simulations were run for the penetration of a 20 mm armour steel plate with a 7.92 mm calibre DS projectile. The analysis led to the following conclusions:

- the numerical analysis runs allowed a classification of the main failure mechanisms and stages of the armour plate by impact of the DS projectile. Decisive to the high penetrating capability of the DS projectiles were the non-optimized properties of armour steel (its high brittleness) and high kinetic energy of the projectile, which generated high shearing stresses upon impact against the steel slab causing the effect of 'plugging' upon penetration;
- what was proven was the high combat effectiveness of the DS projectile and the reference source information by which the DS projectile could pierce a 20 mm thick armour plate made from the material applied during the World War II era;
- high effectiveness of the ALE formulation of elements in describing plastic materials subject to high strain at high strain rates was confirmed.

FUNDING

The author received no financial support for the research, authorship, and/or publication of this article.

REFERENCES

[1] Schultz Walter. 2011. *1000 ręcznej broni palnej*. Ożarów Mazowiecki: Wydawnictwo Olesiejuk.
[2] Bishop Chris. 1998. *The Encyclopedia of Weapons of World War*. London: Barnes & Noble Books.
[3] http://www.winterwar.com/Weapons/FinAT/FINantitank2
[4] Klorek Mikołaj. 2016. „Najpierw był pocisk – karabin przeciwpancerny kb. wz. 35 UR". www.polska-zbrojna.pl (last accessed in January 2018).
[5] Mackiewicz Michał. 2018. „Karabiny przeciwpancerne". www.polska1918-89.pl (last accessed in January 2018).
[6] Gwóźdź Zbigniew, Piotr Zarzycki. 1993. *Polskie konstrukcje broni strzeleckiej*. Warszawa: Wydawnictwo Sigma Not.
[7] Yoffa N., A. Hurlich. 1945. *Metallurgical Examination of Armor and welded joints from the side of a German PzKw (Panther) Tank, Experimental report*. Watertown Arsenal Laboratory, USA.
[8] Riffin P.V. 1945. *Metallurgical Examination of a 3 ¼" Thick armor plate from German PzKw (Panther) Tank, Experimental report*. Watertown Arsenal Laboratory, USA.
[9] Johnson G.R., W.H. Cook. 1983. A constitutive model and data for metals subjected to large strains and high temperatures. In *Proceedings of the 7th Symposium on Ballistics*. Hague, The Nederlands.
[10] *LS-DYNA® Keyword User's Manual, Volume II Material Models*. 2016. Livermore Software Technology Corporation, USA, www.lstc.com.
[11] Rosenberg Zvi, Erez Dekel. 2012. *Terminal Ballistics*. Springer.
[12] *HyperMesh 2017 User Guide*. 2017. Altair Engineering, Inc.
[13] *LS-DYNA® Keyword User's Manual, Volume I*. 2016. Livermore Software Technology Corporation, USA, www.lstc.com.
[14] Shah H. Quasim, Hasan M. Abid. 2011. *From LS-Prepost to LS-Dyna: An introduction*. LAP Lambert Academic Publishing GmbH & Co, KG.
[15] *ANSYS AUTODYN v. 16- The interactive non-linear dynamic analysis code. Software materials library*

Karabin przeciwpancerny wz. 35 „Ur” – analiza numeryczna procesu penetracji opancerzenia czołgu z okresu II wojny światowej

Mariusz MAGIER[1], Paweł ŻOCHOWSKI[1], Wojciech BURIAN[2]

[1]Wojskowy Instytut Techniczny Uzbrojenia,
ul. Prymasa Stefana Wyszyńskiego 7, 05-220 Zielonka
[2]Sieć Badawcza Łukasiewicz – Instytut Metali Nieżelaznych
ul. Sowińskiego 5, 44-100 Gliwice

Streszczenie. W artykule zaprezentowano wyniki symulacji procesu penetracji, płyty stalowej, o parametrach wytrzymałościowych zbliżonych do opancerzenia czołgów z okresu II wojny światowej, przez pocisk typu DS, wystrzelony z 7,92 mm karabinu przeciwpancernego wz.35 „Ur”. Podstawowe parametry techniczne, niezbędne do procesu symulacji, uzyskano ze źródeł historycznych. Dzięki zastosowaniu metody elementów skończonych (Ls-Dyna) oszacowano zdolność penetracji pociskiem DS dla wybranych prędkości uderzenia w pancerz. Decydujący wpływ na wysoką skuteczność pocisków DS miały niezoptymalizowane właściwości stali pancernej (wysoka kruchość) oraz wysoka energia pocisku skutkująca generowaniem dużych naprężeń ścinających, powodujących wybijanie korka z pancerza. Na podstawie wyników symulacji potwierdzono wysoką skuteczność pocisku DS oraz tezę, że wspomniany pocisk był w stanie przebić 20 mm płytę wykonaną z ówczesnej stali pancernej.
Słowa kluczowe: karabin przeciwpancerny, pancerz, balistyka końcowa, metoda elementów skończonych